



## Section 4. Transport

DOI:10.29013/AJT-24-3.4-51-55



### WAYS TO CONTROL AND REDUCE HIGH-FREQUENCY LOADS IN OFF-ROAD VEHICLES

*Tamaz Morchadze*<sup>1</sup>, *Nunu Rusadze*<sup>1</sup>

<sup>1</sup> Faculty of Technical Engineering, Akaki Tsereteli State University, Kutaisi, Georgia

---

**Cite:** Morchadze T., Rusadze N. (2024). Ways to control and reduce high-frequency loads in off-road vehicles. *Austrian Journal of Technical and Natural Sciences* 2024, No 3–4. <https://doi.org/10.29013/AJT-24-3.4-51-55>

---

#### Abstract

The paper presents the vibroacoustic control method, and in particular, the following issues are discussed: diagnosis, control, and ways of reducing high-frequency loads in off-road vehicles; determination of optimal clutch damper parameters; improving the design of the transport shaft, and reduction of vibroactivity in the gear transmissions.

**Keywords:** resonance; diagnosis; control; vibroacoustics; damper; stiffness; cardan

#### Introduction

Throughout the history of the automotive industry, the reduction in load on parts and components of the vehicle as a factor determining reliability has always been of great importance. In this direction, there is an imperative need to intensify the research work at the modern stage, when the production of motor vehicles is rising mainly by increasing the carrying capacity and using high-power internal combustion engines. In such engines, the load mode of the main parts and components of the vehicle, including the transmission, increases. This process requires a more in-depth study of the high-frequency dynamic load of the transmission.

#### Method

Based on all of the above, it is important to use the vibroacoustic control method to diagnose the technical condition caused by the high-frequency dynamic loads of the vehicle transmission.

To reduce high-frequency dynamic loads, it is necessary:

- to determine optimal clutch damper parameters;
- to improve the design of the transmission shaft;
- to reduce vibroactivity in a gear transmission.

There are many analytical and graphoanalytical methods for calculating the torsional vibration damper in the vehicle transmission. In the case when the damper is placed in the clutch and it is not possible to install it

in another place, good results are achieved by the method proposed by Professor P. Lukin (Prof. P. P. Lukin., 1982).

Figure 1 illustrates the dynamic scheme of the vehicle transmission. The a-c link equivalent stiffness and damping coefficients are calculated by the formula:

$$C_{eq} = \frac{F_{max}(\alpha_1, \alpha_2)}{\lambda_1} = \frac{C_{2-4}}{C_1 + C_{2-4}} \left( C_1 + \frac{M_T}{\lambda_1} \right) \quad (1)$$

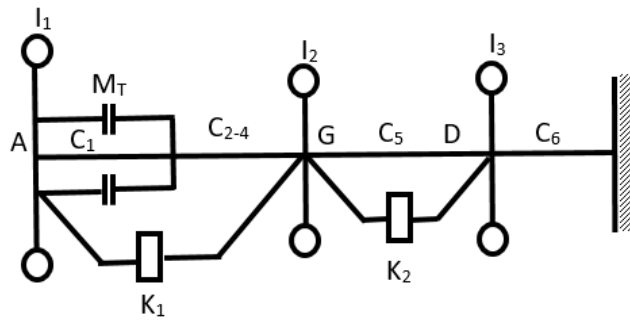
$$K_{eq} = \frac{4 \cdot M_T (C_{2-4} \lambda_1 - M_T)}{\pi \lambda_1^2 \omega_3 (C_1 + C_{2-4})} \quad (2)$$

$C_{eq}$  and  $K_{eq}$  coefficients are non-linear functions of the ratio  $\frac{M_t}{\lambda_1}$ . In addition,  $K_{eq}$  is dependent on  $\omega_v$  vibration frequency (Bugaru, M. & Vasile, A., 2022).

Using the obtained coefficients, we determine the system's natural vibration frequencies. The implication is that  $\alpha_1 = \lambda_1 \sin \omega t$  and  $\alpha_2 < \lambda_2 \sin \omega t$ . The amplitude  $\lambda_1$  is calculated as follows:

$$\lambda_1 = (1 + ih) \frac{M_t}{C_{2-4}}, \text{ where } i=1,2,3\dots, n, h = 0.25.$$

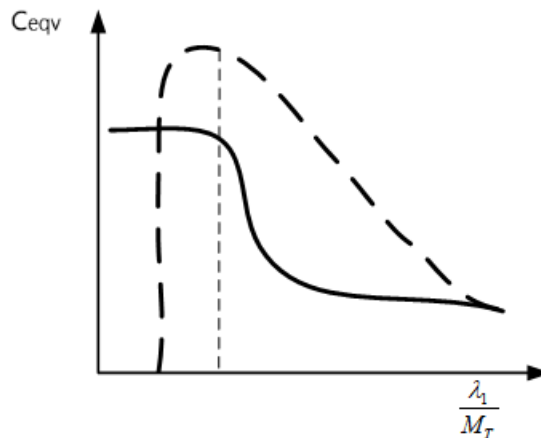
**Figure 1.** The dynamic scheme of the vehicle transmission



Due to the fact that damping has a negligible effect on natural vibration frequency, when calculating the coefficients  $K_{eq}$ , their corresponding natural frequencies ( $K = K_1 + K_{eq} = 0$ ) are used. Then, taking into account  $K$  coefficients, it is possible to accurately calculate natural vibration frequencies. (Rusadze, T., & Iejava, A., & Cirekidze, G. & Feradze, M. & Mamaladze, T. & Gvinianidze, N. 1998).

Figure 2 and Figure 3 show the dependence of the coefficients  $C_{eq}$  and  $K_{eq}$  on the ratio  $\frac{K_1}{M_T}$ . It can be seen that  $K_{eq}$  has a maximum for the value of  $\left( \frac{\lambda_1}{M_T} \right)$ , at which the largest value of the vibrational energy is dissipated (Bugaru, M. & Vasile, A., 2021)

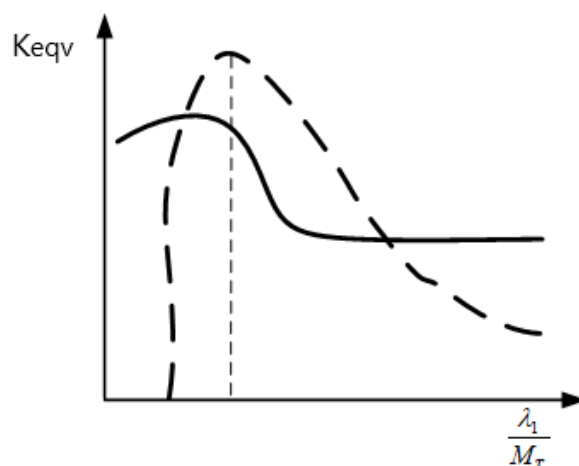
**Figure 2.** The dependence of the coefficient  $C_{eq}$  on the ratio of  $\frac{K_1}{M_T}$



According to the results of the calculation of the natural vibration frequencies of the resonance being studied, a diagram (Fig. 3)

of the different stiffness and friction moments of the damper is constructed.

**Figure 3.** The dependence of the coefficient  $K_{eq}$  on the ratio of  $\frac{K_1}{M_T}$



In cars and trucks, as well as in some buses, transmission shafts are often used.

Often, in the construction of the transmission shaft, the peculiarities of its operation are not taken into account, in particular, when it has an excess mass that causes vibration in the transmission. (Rusadze, T. P. & Platonov, V. F. & Semenov, V. M. & Gogitidze, A. S. & Rusadze, P. T., 2002).

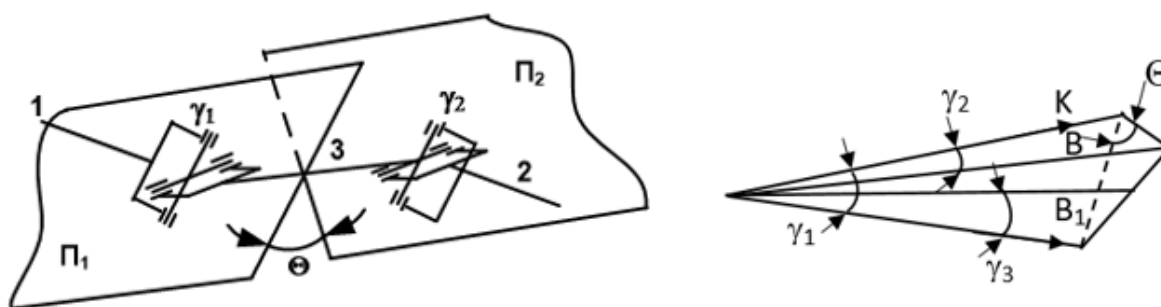
Various new transmission shaft designs to provide the required strength can be based on optimality criteria such as mass, cost, and maximum operational efficiency.

To create a new transmission shaft, we consider it appropriate to correct the angles of hinges of unequal angular speeds and to use hinges of equal angular speeds in the design.

Based on the concept obtained, we developed a new version of the transmission shaft.

Hinges of equal angular speeds and a tube made of composite material were used in the design. The clutch shaft, the primary gearbox shaft, and the transmission shaft itself are not located in the same plane, which causes additional excitation of torsional vibrations due to features of the kinematics of universal joints.

**Figure 4.** A scheme of the double-hinged spatial cardan drive



On the general scheme of the double-hinged spatial cardan drive shown in Figure 4, the plane  $\Pi_1$  passes through the drive (1) and cardan (3) shafts, while the plane  $\Pi_2$  passes through the cardan (3) and driven (2) shafts. If we denote the turning angles of the drive and driven forks of the first joint by  $\phi_3$  and  $\phi'_3$ , and the angles of the forks of the second joint by  $\phi_4$  and  $\phi'_4$ , then according to: (Florian Ion Tiberiu Petrescu, & Rely Victoria Virgil Petrescu, 2019).

$$\phi'_4 = \phi_4 - \lambda_2 \sin 2(\phi_4 + \Theta) + \lambda_2 \sin 2\Theta. \quad (3)$$

In order to reduce torsional vibrations in the double-hinged spatial cardan drive, it is not viewed as necessary to put the angle  $\Theta$  in the equation. This requirement would be achieved if we set the forks of the cardan shaft in the initial position and perpendicular to the planes  $\Pi_1$  and  $\Pi_2$ ; that is, we will turn the forks at an angle of  $\Theta$ , or we will turn one of the forks at an angle of  $\Theta$  towards the other. In this case, no longer terms containing the angle  $\Theta$  are created in the bond equation because,

after the turn, the reference plane of the angle  $\phi_4$  coincides with the plane  $\Pi_2$ . In the differential equation of torsional vibrations, there will no longer be additional terms containing the angle  $\Theta$  and it will have the same structure as a “flat” double-hinged cardan drive. That is, in the case of turning forks, the optimal angles for setting a smooth double-hinged cardan drive can be selected under the same conditions as in the case of a “flat” cardan drive.

The angle  $\Theta$  shall be calculated analytically at the angle between the setting angles  $\gamma_1$  and  $\gamma_2$  and the drive and driven shafts ( $\gamma_3$ ).

$$\cos \Theta = \frac{\cos \gamma_3}{\sin \gamma_1 \sin \gamma_2} - \operatorname{ctg} \gamma_1 \cdot \operatorname{ctg} \gamma_2. \quad (4)$$

In the special case, when the cardan drive is “flat”, that is, a plane can be drawn on all three vectors, then by inserting the value of  $\gamma_3$  into the equation, we will obtain that  $\cos \Theta = 1$ , or  $\Theta = 0$ .

If, as a result of the calculation, the value of the angle  $\Theta$  according to the above formula (4) is obtained with a negative sign, which corresponds to an obtuse angle, then the drive fork of the second joint lags behind the plane  $\Pi_2$  during rotation, and it must turn at an angle  $\Theta$  in the direction of rotation of the cardan drive, or vice versa, the driven fork of the first joint must turn in the direction opposite to the rotation of the cardan drive (<https://www.researchgate.net/>).

If the result in equation (4) is obtained with a positive sign, in this case, the drive fork of the second joint turns in front of the plane  $\Pi_2$ , and it must turn at an angle  $\Theta$  in the direction opposite to the rotation of the cardan drive (or the driven fork of the first joint must turn in the direction of the rotation of the cardan drive).

In this case, when  $\gamma_1 = 2^{\circ}39'40''$ ,  $\gamma_2 = 3^{\circ}34'11''$ , and  $\gamma_3 = 5^{\circ}$ , we obtain  $\Theta = 87^{\circ}04'$ .

When  $\gamma_1 = 3^{\circ}04'540''$ ,  $\gamma_2 = 3^{\circ}06'44''$ , and  $\gamma_3 = 5^{\circ}$ ,  $\Theta = 86^{\circ}45'$ .

That is, the driven fork of the first joint must be rotated in the direction of rotation of the cardan drive at an angle of  $87^{\circ}04'$  in the

case of an angular structure, or at an angle of  $86^{\circ}45'$  by changing the installation angles.

Both straight and helical gears are used in off-road vehicle transmissions and gearboxes.

One of the well-known ways to reduce dynamic loads is to increase tooth deformation when entering the coupling phase, which would be achieved by increasing overall tooth compliance or increasing compliance at the coupling points (for example, increasing tooth height or reducing tooth cross-section).

### Result

The excitation of vibrations in the straight-toothed gears is a powerful source of the periodic change in stiffness according to the coupling phase. If we assume that the stiffness of coupling is proportional to the total length of the contact lines, then it is possible to achieve constancy in the total length of the lines in the straight-toothed gear.

In a helical gear, the stiffness is constant according to the coupling phase, if the helical overlap factor is an integer. However, despite the product of the area of the tooth crown on the axial pitch, there is still a second source of vibration – the error of the toothed gear wheels on the circular pitch, which causes the teeth to enter the non-working point, or out of the coupling line.

The method of mutual compensation of the exciting forces is known, the essence of which is the rational selection of the phase between the two mentioned factors – the change of the hardness of the teeth according to the coupling phase, and not the periodic entry of the teeth into the working point.

### Discussion

In order to reduce the dynamic forces, it is also possible to make the gear with a composite structure. The elastic element installed between the gear hub and the rim will resist the propagation of vibration, and due to the elastic-damping properties, the vibroacoustic characteristics of the gear transmission will be improved.

## References

- Rusadze, T. lejava, A. cirekidze, G. Feradze, M. Mamaladze, T. Gvinianidze, N. (1998). Vehicle loading modes and reliability. Georgia, – Kutaisi. –296 p.
- Rusadze, T. P. Platonov, V. F. Semenov, V. M. Gogitidze, A. S. Rusadze, P. T. (2002). Optimization of vehicle parameters. ALIONI, Georgia, – Batumi. – 319 p.
- Report on research work on “Study of torsional vibrations in the transmission of a front-wheel drive vehicle and optimization of the parameters of the damper device”. MAMI. Scientific advisor, Prof. P. P. Lukin. 1982. UDC629-\*114.:6:-752. Registration 81069443
- Bugaru, M. Vasile, A (2022, 10, 10). A Physically Consistent Model for Forced Torsional Vibrations of Automotive Driveshafts. 2–21. URL: <https://doi.org/10.3390/computation10010010>
- Bugaru, M. Vasile, A. (2021). Nonuniformity of Isometric Properties of Automotive Driveshafts. Computation 2021. – 9, 145. – P. 2–13. <https://doi.org/10.3390/computation9120145>
- Florian Ion Tiberiu Petrescu. Rely Victoria Virgil Petrescu. The Structure, Geometry, and Kinematics of a Universal Joint. – P. 1713–1723. URL: <http://www.ijmp.jor.br/> V. 10. – N. 8. Special Edition Seng 2019. ISSN: 2236-269X. DOI:10.14807/ijmp.v10i8.923. URL: <http://creativecommons.org/licenses/by/3.0/us>
- URL: [https://www.researchgate.net/publication/362644644\\_Book\\_3-BREN\\_PUBLISHER](https://www.researchgate.net/publication/362644644_Book_3-BREN_PUBLISHER)

submitted 10.04.2024;  
accepted for publication 24.04.2024;  
published 23.05.2024  
© Morchadze T., Rusadze N.  
Contact: [nunu.rusadze@atsu.edu.ge](mailto:nunu.rusadze@atsu.edu.ge)